Supporting information

Efficient small molecule bulk heterojunction solar cells with high fill factors via introduction of π -stacking moieties as end group

Guangrui He,[1] Zhi Li,[1] Xiangjian Wan,[1] Jiaoyan Zhou,[1] Guankui Long,[1] Shuzhong Zhang,[2] Mingtao Zhang,[3] Yongsheng Chen[1,*]

Table S1. d-Spacing values of the conjugated molecules.

Compounds	d_{100} (Å)	Intensity of (100)	FWHM	d_{200} (Å)	d_{300} (Å)
D2R(8+2)7T	--			--	--
DTDMP7T	19.0	1204	0.0073	--	--
DERHD7T	19.3	3894	0.0026	9.6	6.4
DCAO7T	21.0	5154	0.0030	10.5	7.0
DIN7T	19.3	20761	0.0031	9.7	6.5
DINCN7T	17.4			8.3	--
DDIN7T	--			--	--

Table S2. Intensity values and Domain size (estimated from (FWHM) via Scherrer equation)

Compounds	d_{100} (Å)	2θ（degree）	Intensity of (100)	FWHM （degree）	Domain size
DTDMP7T	19.0	4.66	1204	0.42	19nm
DERHD7T	19.3	4.51	3894	0.21	37nm
DCAO7T	21.0	4.20	5154	0.18	44nm
DIN7T	19.3	4.58	20761	0.15	53nm

Table S3. Summary of device performance for various BHJ devices based on DDIN7T.

Active Layer	W/W	Voc / V	Jsc / mA cm^{-2}	FF (%)	PCE (%)
DDIN7T : $PC_{61}BM$[b]	8/4	0.76	1.28	0.26	0.24
DDIN7T : $PC_{61}BM$[b]	8/8	0.76	2.12	0.27	0.44
DDIN7T : $PC_{61}BM$[b]	8/11.4	0.76	1.66	0.26	0.33
DDIN7T : $PC_{61}BM$[b]	8/15	0.74	1.22	0.30	0.27
DDIN7T : $PC_{61}BM$[b] with 0.2% (v/v) CN	8/8	0.72	1.67	0.25	0.31
DDIN7T : $PC_{61}BM$[a]	8/8	0.76	3.14	0.28	0.66

a: device with Ca/Al as cathode; b: device with LiF/Al as cathode.

Table S4. Summary of device performance for various BHJ devices based on DIN7T in the work using LiF/Al as cathode.

Active Layer	W/W	Voc / V	Jsc / mA cm^{-2}	FF (%)	PCE (%)
DIN7T : $PC_{61}BM$	8/4	0.80	6.90	72	3.78
DIN7T : $PC_{61}BM$	8/8	0.80	8.21	72	4.71
DIN7T : $PC_{61}BM$	8/10.3	0.80	7.80	70	4.39
DIN7T : $PC_{61}BM$	8/16	0.76	7.30	61	3.37
DIN7T : $ICB_{61}A$	8/8	1.00	4.85	56	2.75
DIN7T : $PC_{71}BM$	8/8	0.80	8.51	69	4.70
DIN7T : $PC_{61}BM$ with 0.3mg/ml PDMS	8/8	0.80	8.56	72	4.93
DIN7T : $PC_{61}BM$ with 0.6mg/ml PDMS	8/8	0.80	7.81	71	4.45
DIN7T : $PC_{61}BM$ with 0.7% (v/v) DIO	8/8	0.50	8.53	31	1.35
DIN7T : $PC_{61}BM$ with 0.2% (v/v) DIO	8/8	0.66	7.69	46	2.37
DIN7T : $PC_{61}BM$ with 0.1% (v/v) DIO	8/8	0.70	9.06	53	3.35
DIN7T : $PC_{61}BM$ with 0.2% (v/v) CN	8/8	0.74	10.10	45	3.37
DIN7T : $PC_{61}BM$ with 0.1% (v/v) CN	8/8	0.76	9.65	59	4.32
DIN7T : $PC_{61}BM$ with 0.05% (v/v) CN	8/8	0.80	8.80	66	4.70
DIN7T : $PC_{61}BM$[a]	8/8	0.78	7.86	69	4.25

a: device with Ca/Al as cathode;

Solubility Measurement

The solubilities of these molecules in CHCl3 were measured optically.

First, a set of standard absorption spectra were taken for these molecules in chloroform at known concentrations (figures S1).

Next, saturated solutions were prepared by mixing an excess of solid material with a small volume of CHCl3, followed by heating and stirring for 2 hours. The mixtures were then allowed to stand for at least 48 hours at room temperature. To ensure that a saturated solution had been acheived, more solid was added to the mixture if excess solid material was not clearly visible in the mixture after the 48 hour period. The saturated and the saturated solutions were next filtered through a 0.45 μm PTFE syringe filter and diluted with 100 to 10,000 volumes of chloroform in order to achieve an optical density within the range of the calibration curves (figures S2).

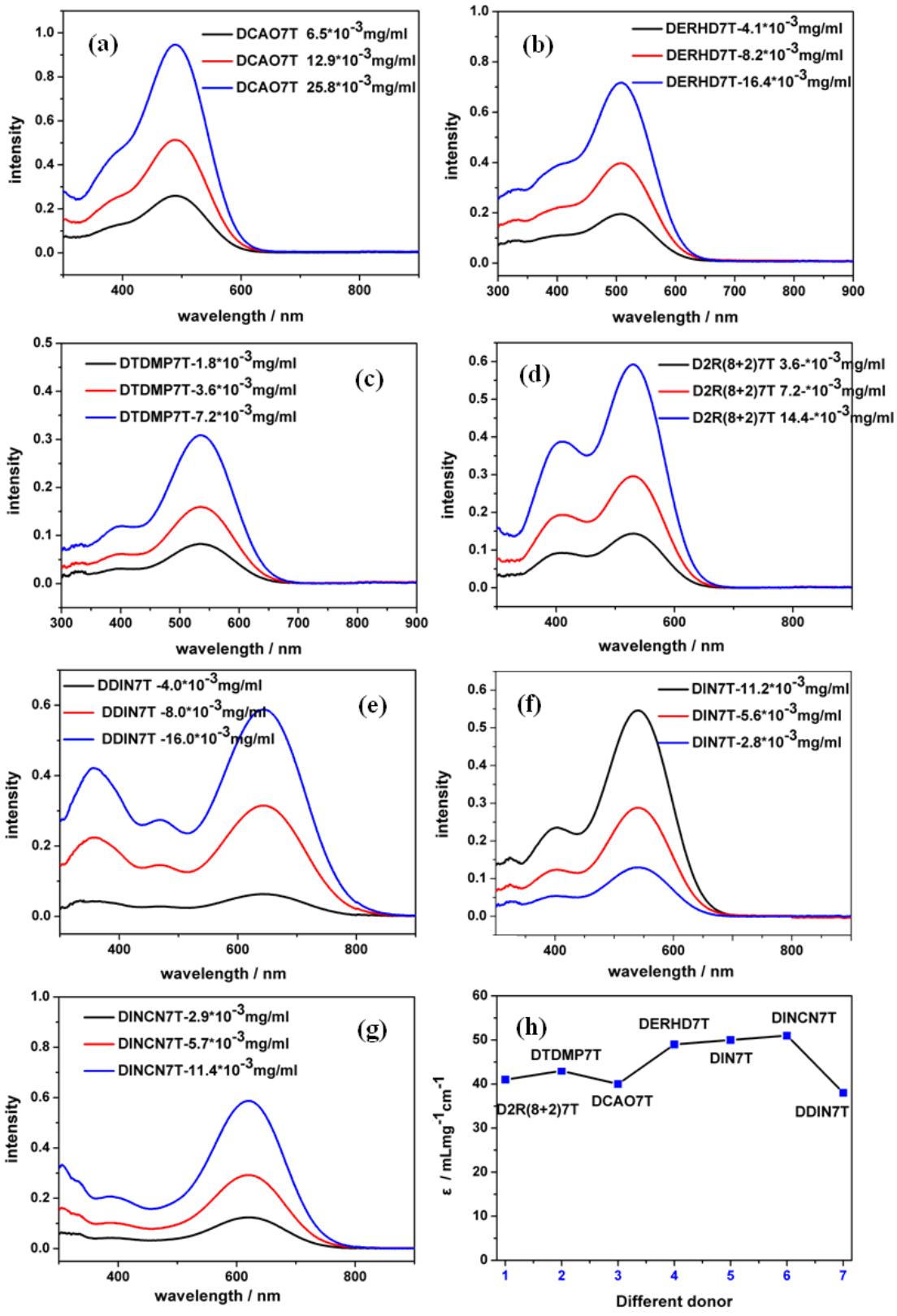

Figure S1: Calibration spectra used to calculate solubility. (a), (b), (c), (d), (e), (f) and (g) Absorption spectra of standard solutions of D2R(8+2)7T, DTDMP7T, DCAO7T, DERHD7T, DIN7T, DINCN7T and DDIN7T respectively. (h) Plot of absorption coefficient at maximum absorption peaks of all these molecules[1].

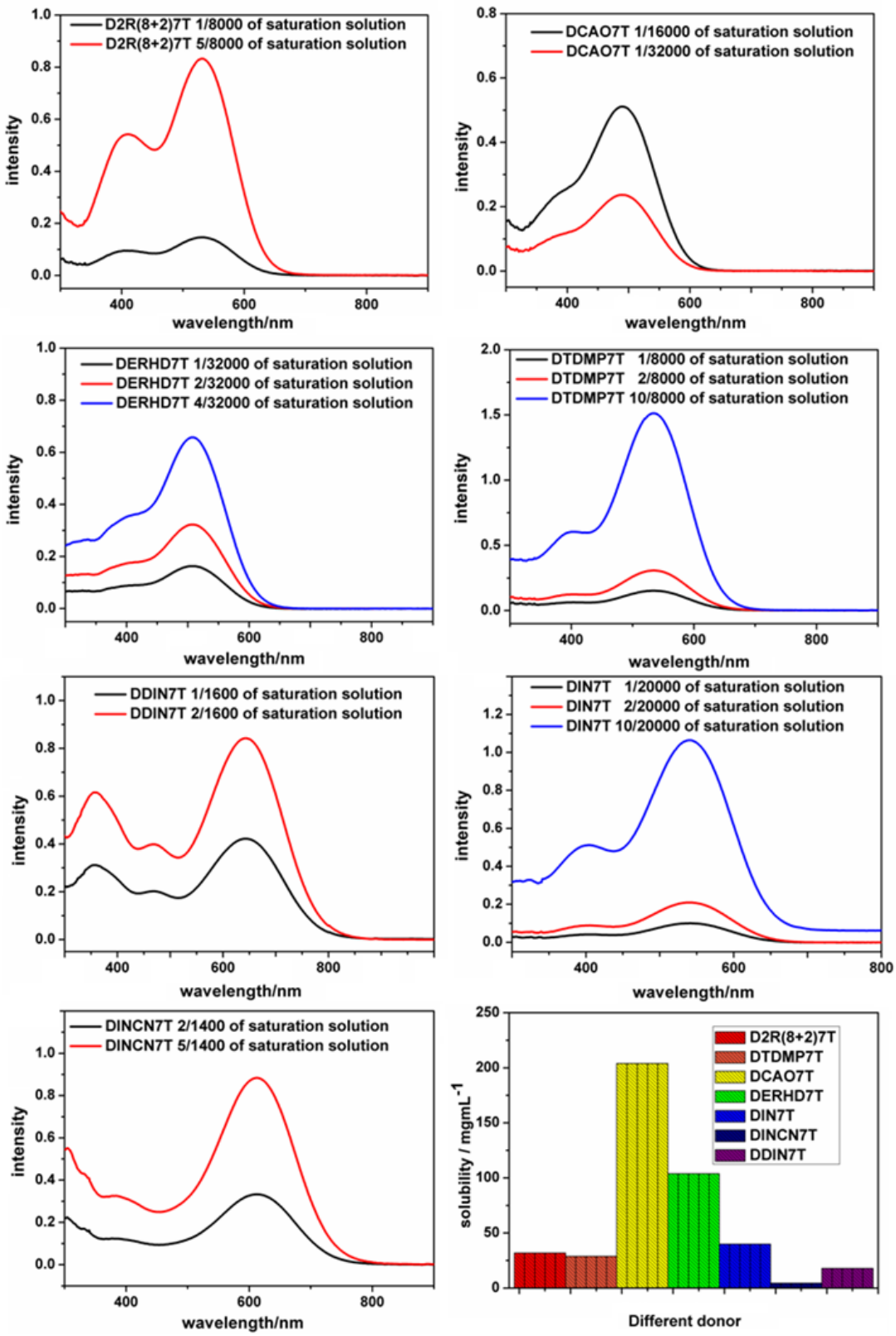

Figure S2: Spectra of the diluted solutions made from the corresponding saturation solution. (a), (b), (c), (d), (e), (f) and (g) absorption spectra of solutions of D2R(8+2)7T, DTDMP7T, DCAO7T, DERHD7T, DIN7T, DINCN7T and DDIN7T respectively. (h) Plot of solubility of all these molecules.

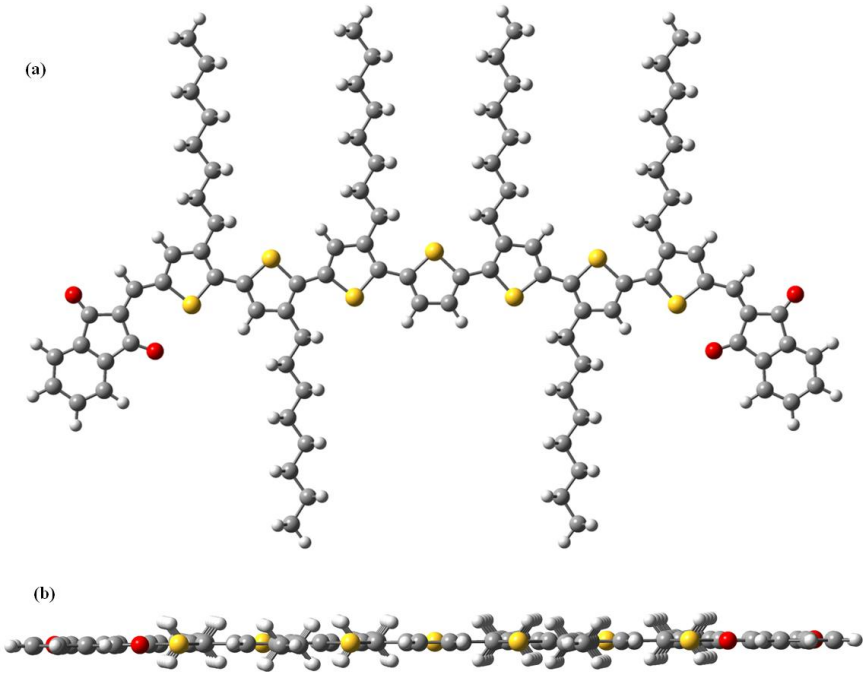

Figure. S3 (a) top view (b) side view of molecular structure of DIN7T. The molecular geometry was optimized by Gaussian09 program, using the Density Functional Theory (DFT) with the PBE1PBE/6-31G(d) basis set and frequency analysis was followed to assure that the optimized structures was stable states[2].

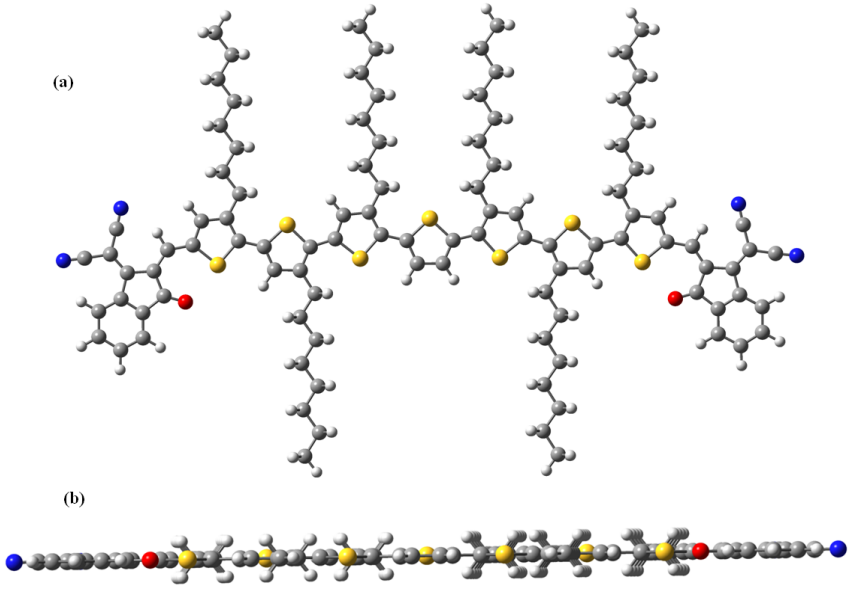

Figure. S4 (a) top view (b) side view of molecular structure of DINCN7T.

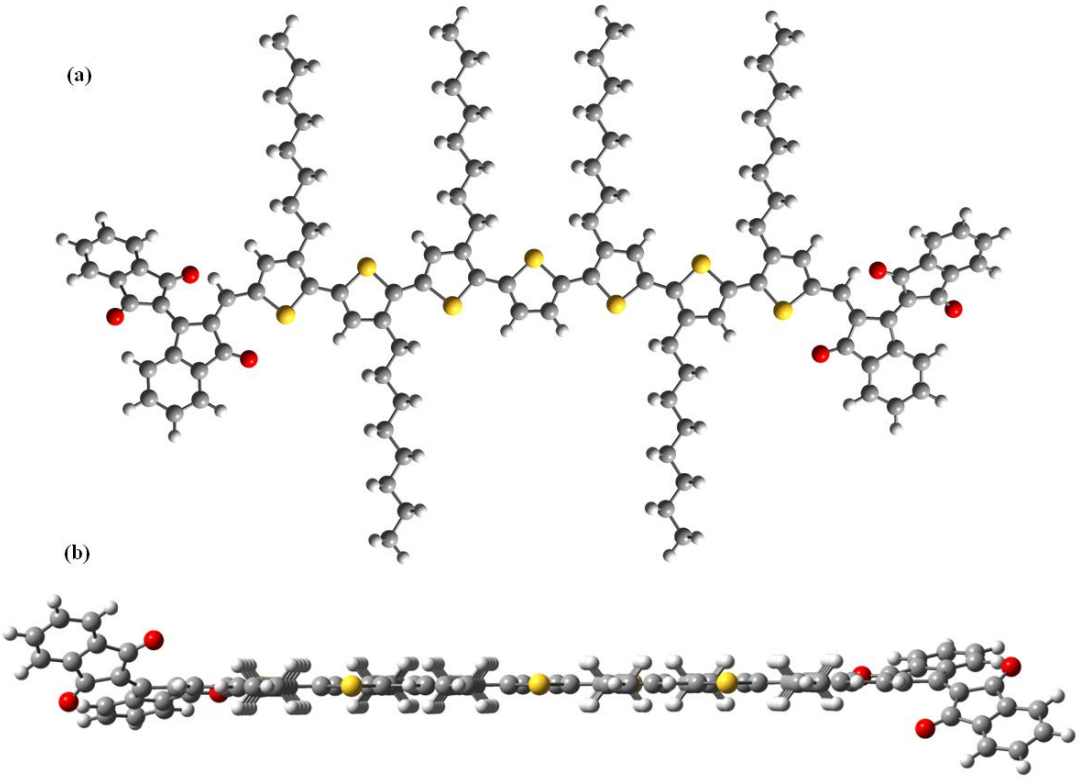

Figure. S5 (a) top view (b) side view of molecular structure of DDIN7T.

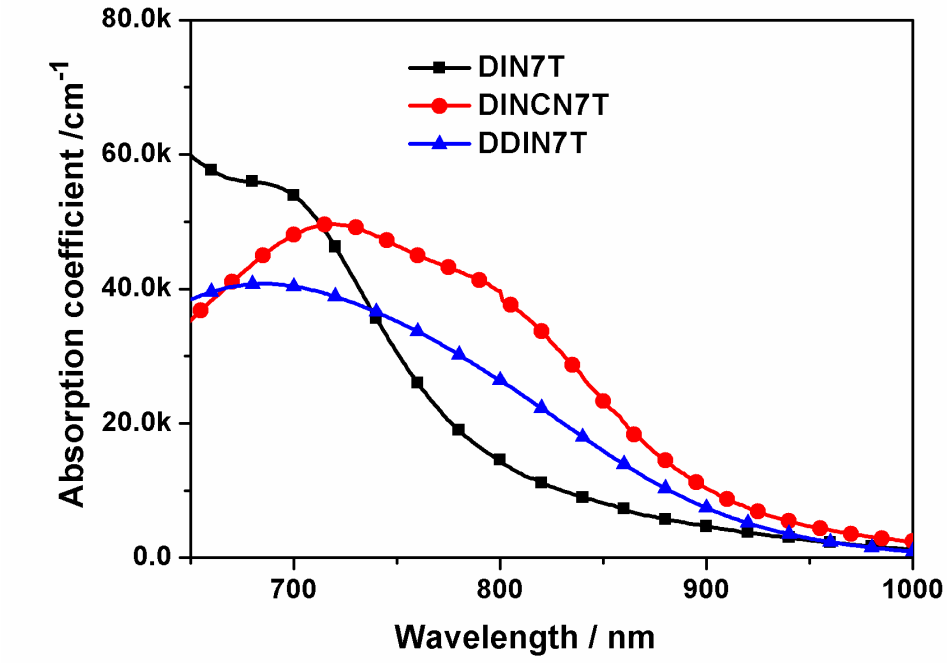

Figure S6. expanded absorption spectra of DIN7T, DINCN7T and DDIN7T as films.

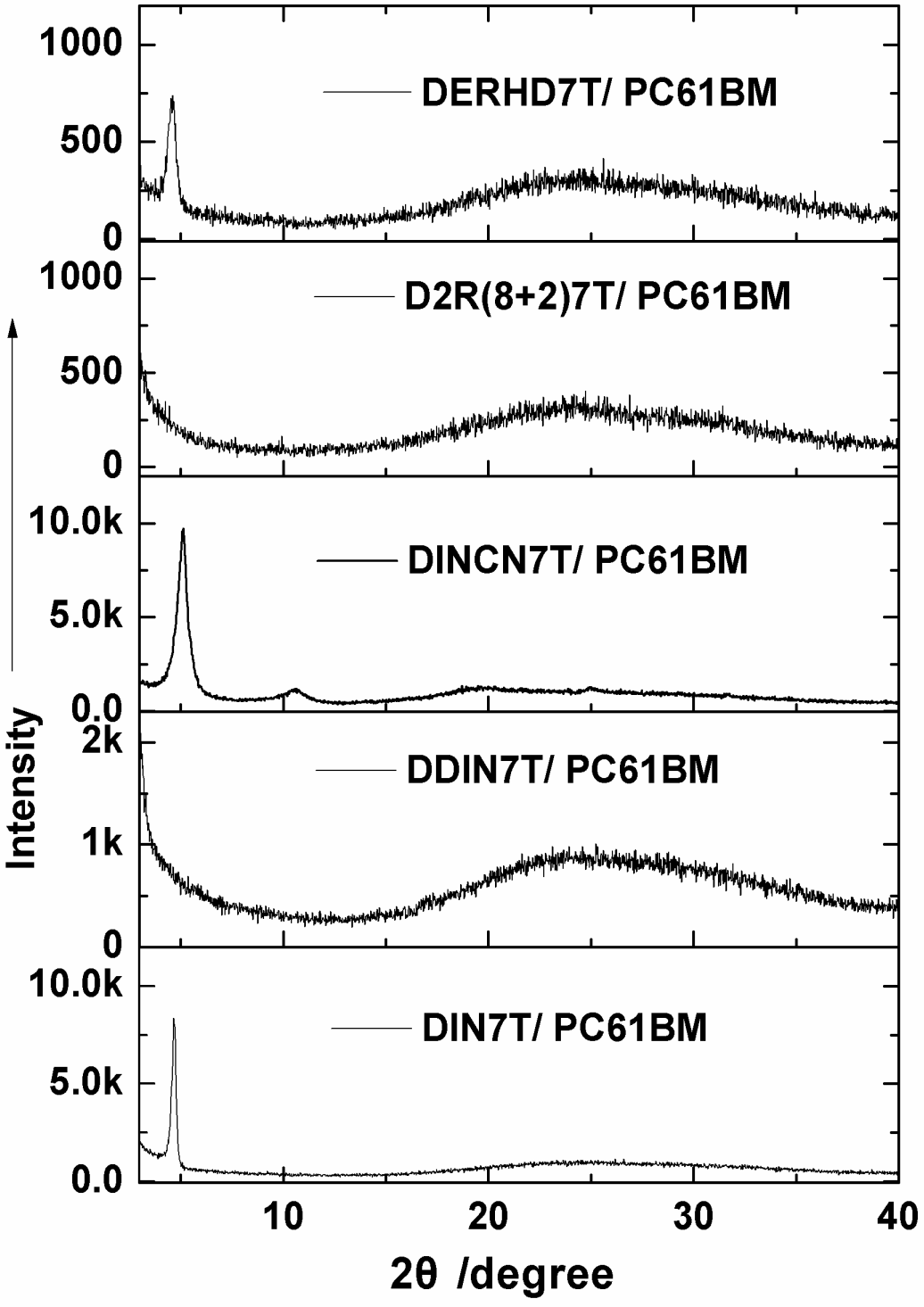

Figure. S7 XRD patterns of DDIN7T/PC61BM, DIN7T/PC61BM, DERHD7T/PC61BM and D2R(8+2)7T/PC61BM films spin-coated from $CHCl_3$ onto glass substrate. DINCN7T/PC61BM film was drop onto glass substrate .

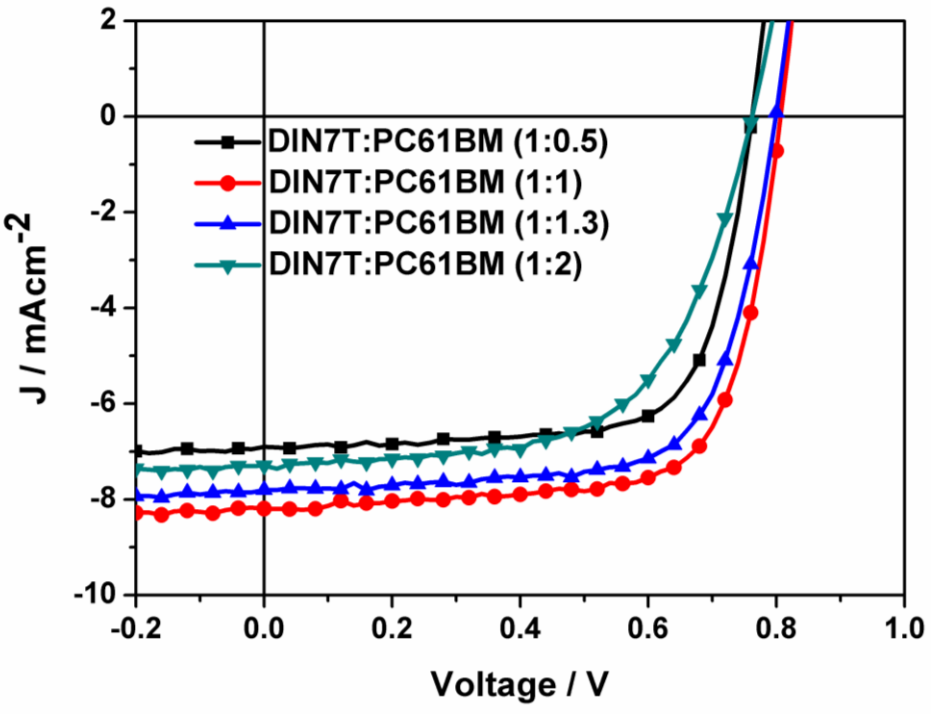

Figure S8. Characteristic J-V curves of BHJ solar cells based DIN7T/PC61BM with different blend ratios (w:w) of 1:0.5, 1:1, 1:1.3 and 1:2 with LiF/Al as the cathode under illumination of AM 1.5 G, 100 mW cm$^{-2.}$

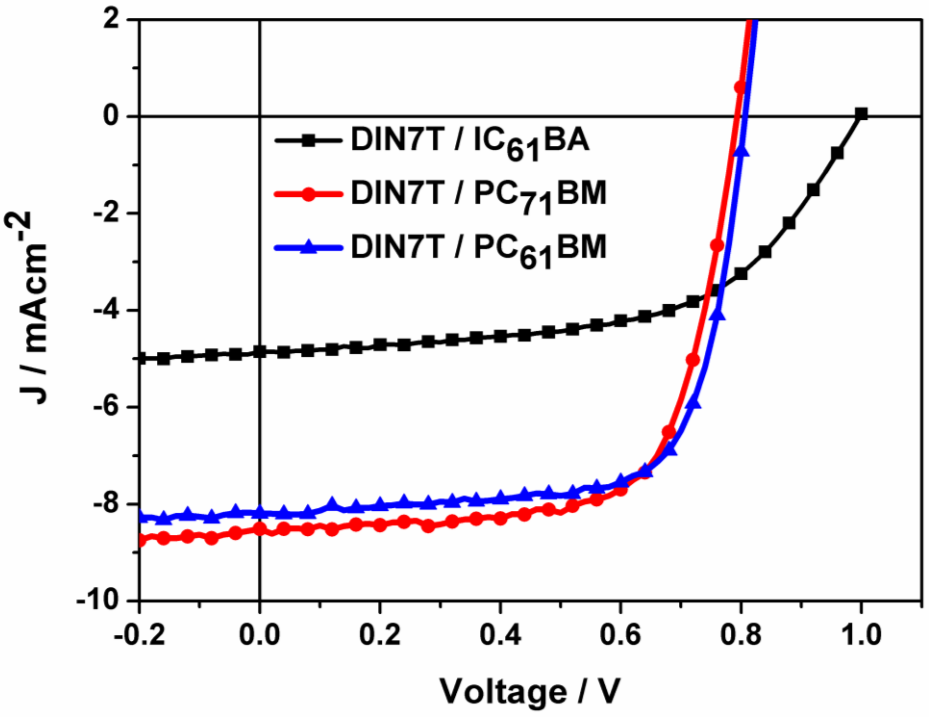

Figure S9. Characteristic J-V curves of BHJ solar cells based DIN7T with different acceptors of IC61BA, PC71BM and PC61BM at (w:w) 1:1 with LiF/Al as the cathode under illumination of AM 1.5 G, 100 mW cm$^{-2.}$

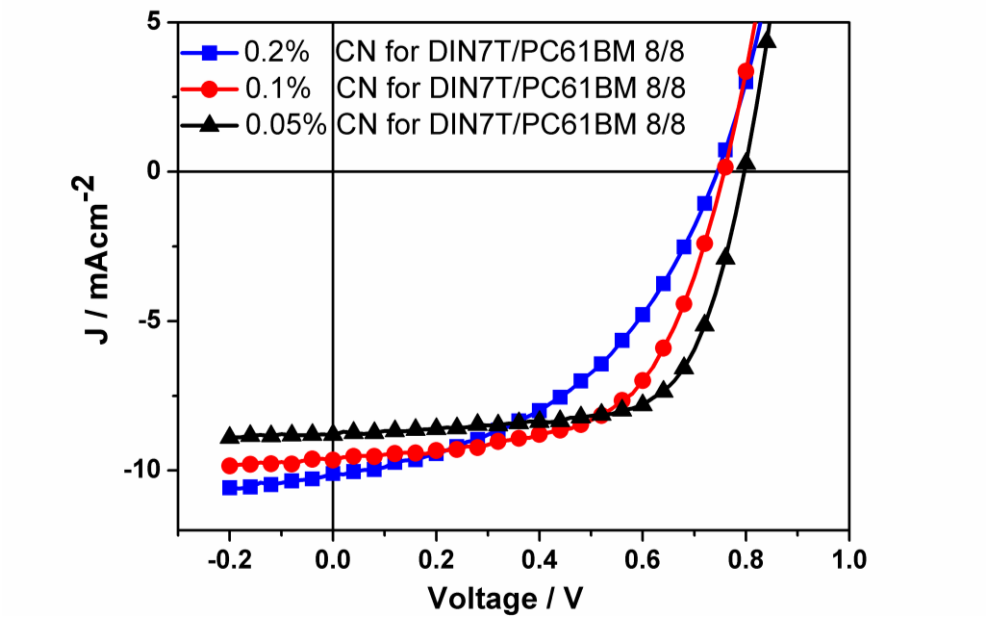

Figure S10. Photovoltaic performance of DIN7T/PC61BM BHJ solar cells with w:w = 1:1 using chloroform solutions when different amount of CN was added.

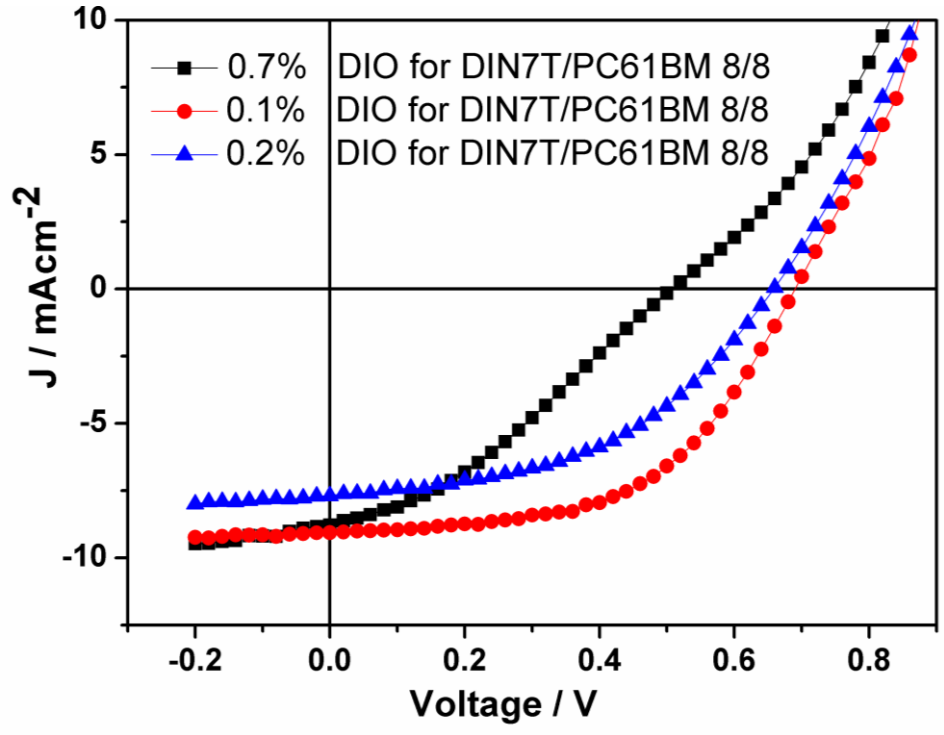

Figure S11. Photovoltaic performance of DIN7T/PC61BM BHJ solar cells with w:w = 1:1 using chloroform solutions when different amount of DIO was added.

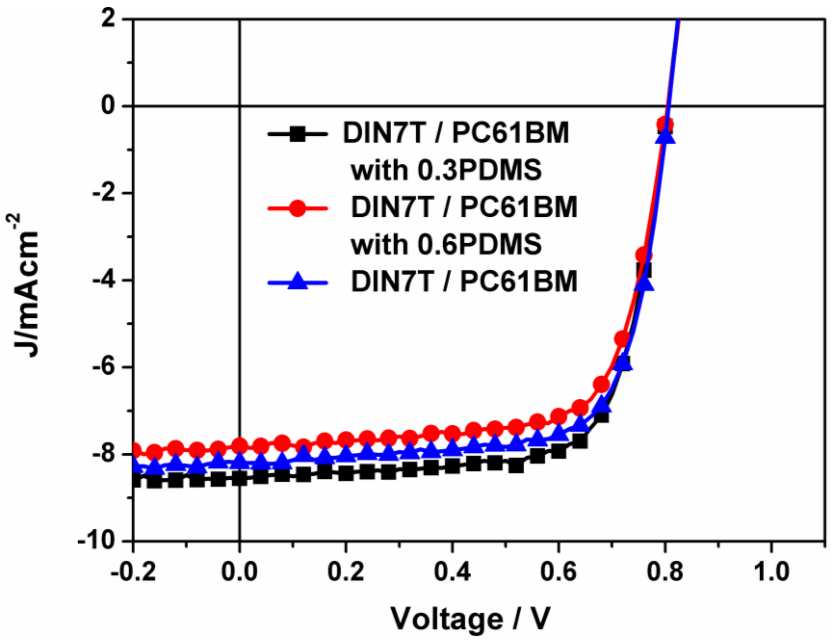

Figure S12. Photovoltaic performance of DIN7T/PC61BM BHJ solar cells with w:w = 1:1 using chloroform solutions when different amount of PDMS was added.

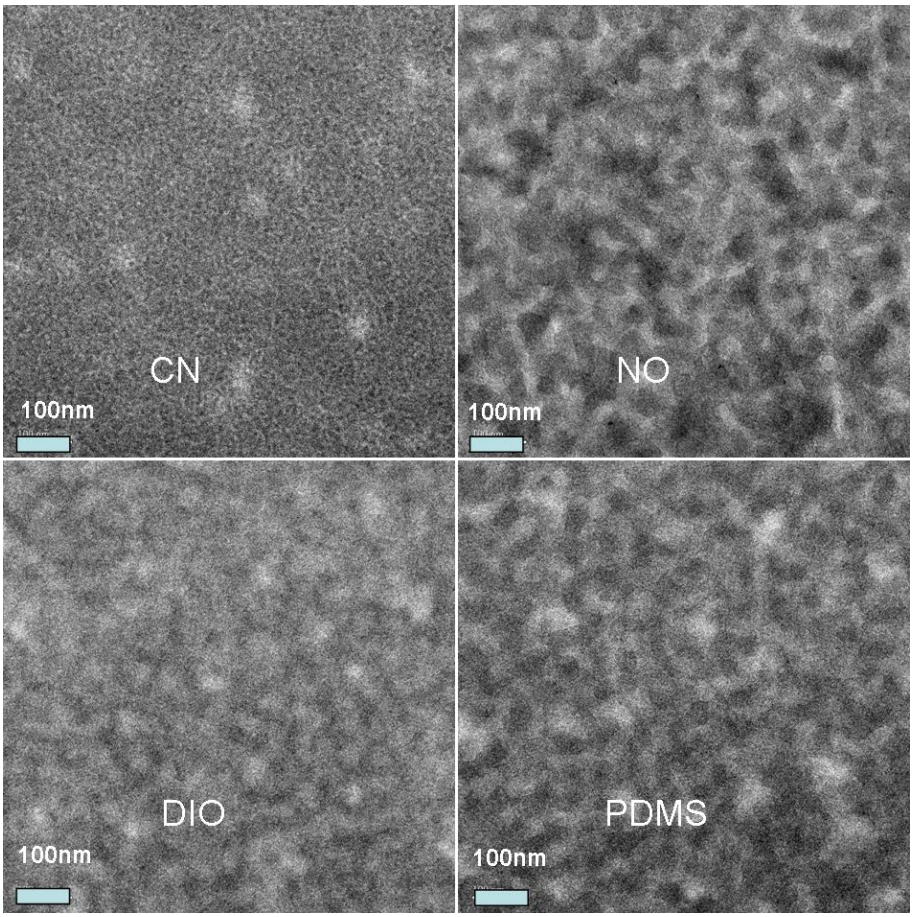

Figure S13. TEM images of DIN7T:PC61BM (1 : 1) devices with (a) 0.2% (V/V) CN, (b) no additive, (c) 0.2% (V/V) DIO, (d) 0.3 mg/mL PDMS.

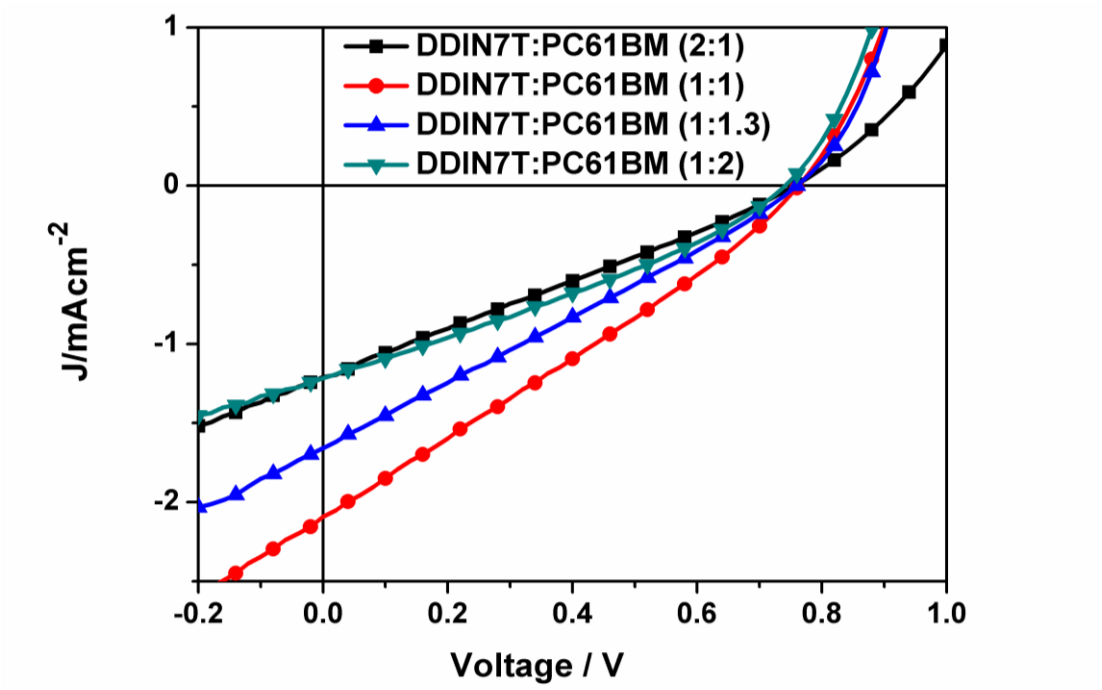

Figure S14. Characteristic *J-V* curves of BHJ solar cells based DDIN7T/$PC_{61}BM$ with blend ratios (w:w) of 1:0.5, 1:1, 1:1.3 and 1:2 with LiF/Al as the cathode under illumination of AM 1.5 G, 100 mW $cm^{-2.}$

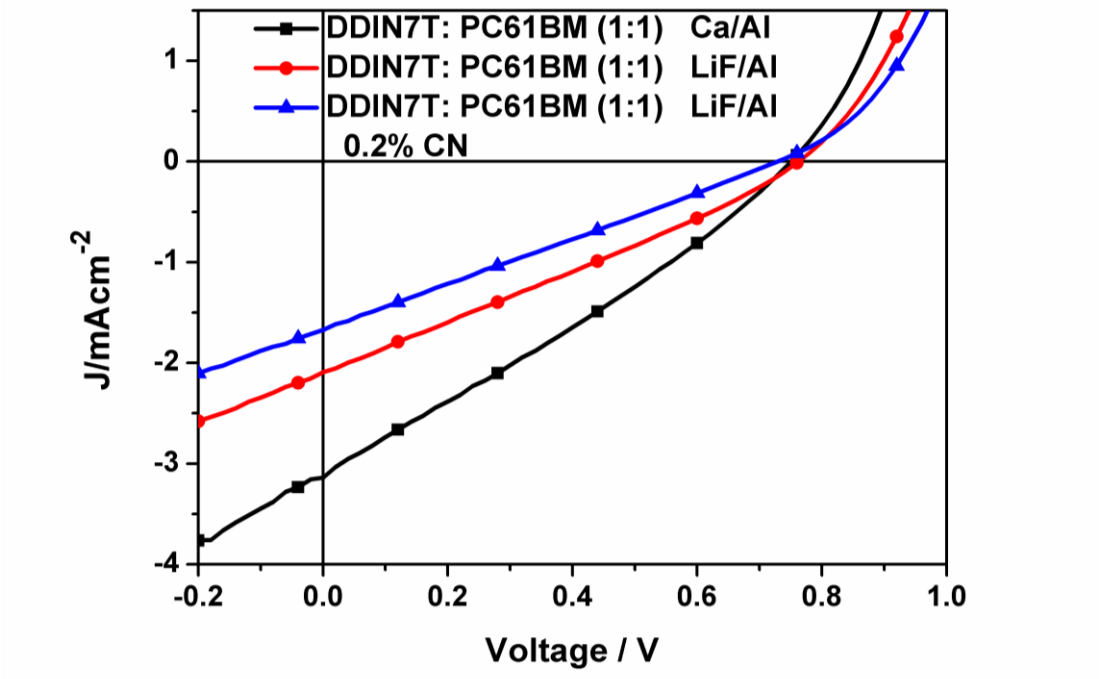

Figure S15. Characteristic *J-V* curves of BHJ solar cells based DDIN7T/$PC_{61}BM$ with blend ratios (w:w) of 1:1 with LiF/Al and Ca/Al as the cathode under illumination of AM 1.5 G, 100 mW $cm^{-2.}$

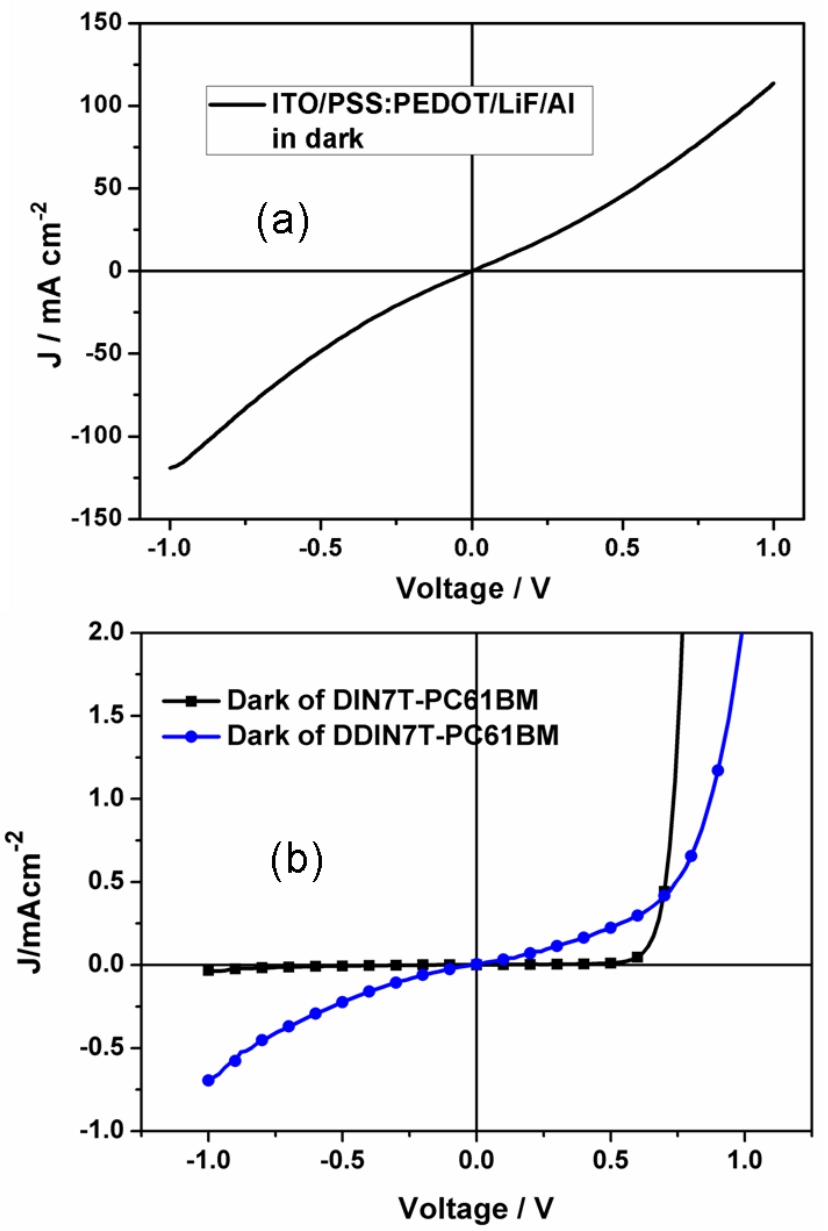

Figure S16. (a) Characteristic *J-V* curves of ITO/PSS:PEDOT/LiF/Al

(b) Characteristic *J-V* curves of BHJ solar cells based DIN7T/PC_{61}BM (1:1) and DDIN7T/PC61BM (1:1) with LiF/Al and Ca/Al as the cathode in the dark.[3]

[3] 1. Compared the J-V curves of Figure S16a and Figure S16b, we can see that the diode is based on the P-N junction formed by the organic donor and acceptor in the active layer.

2. For high crystallinity of DIN7T, it can form a relative pure phase (domain) in the active layer and an efficient P-N junction with PC61BM, which determine the quality of diode. In contrast, DDIN7T based SM-BHJ displayed a bad condition of J-V curve in the dark, for the bad packing situation in the active layer.

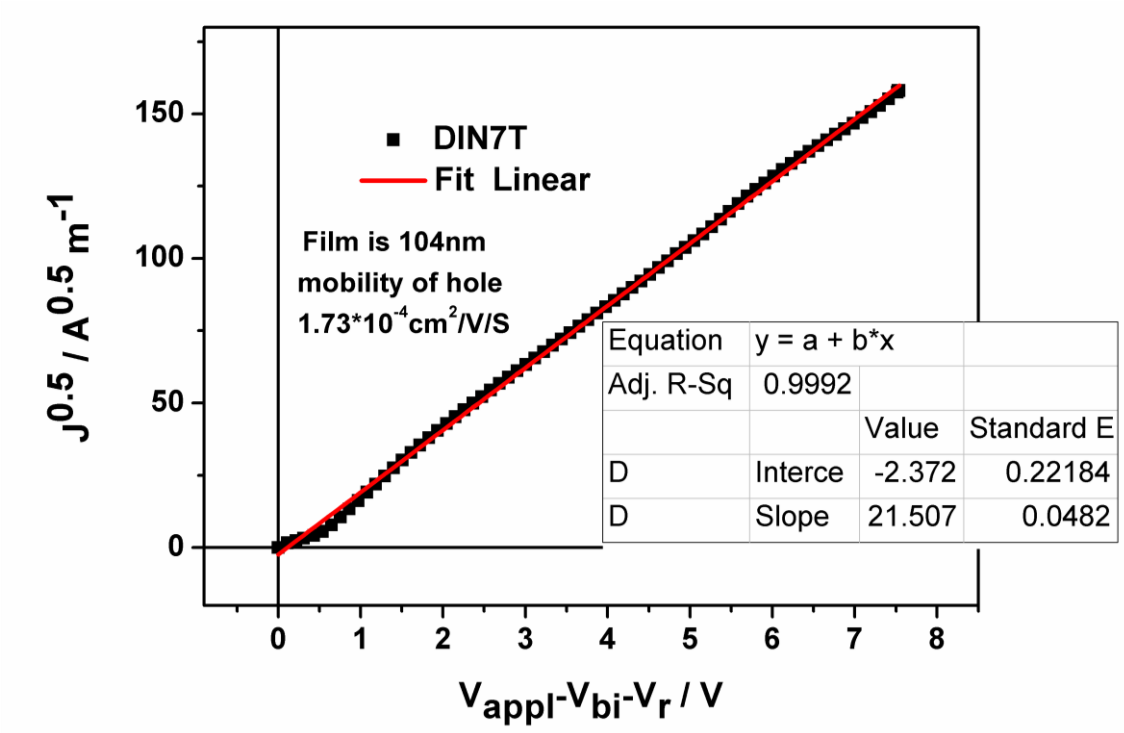

Figure S17. $J^{0.5}$ **vs V plots for the pure DIN7T and DDIN7T film at room temperature.**

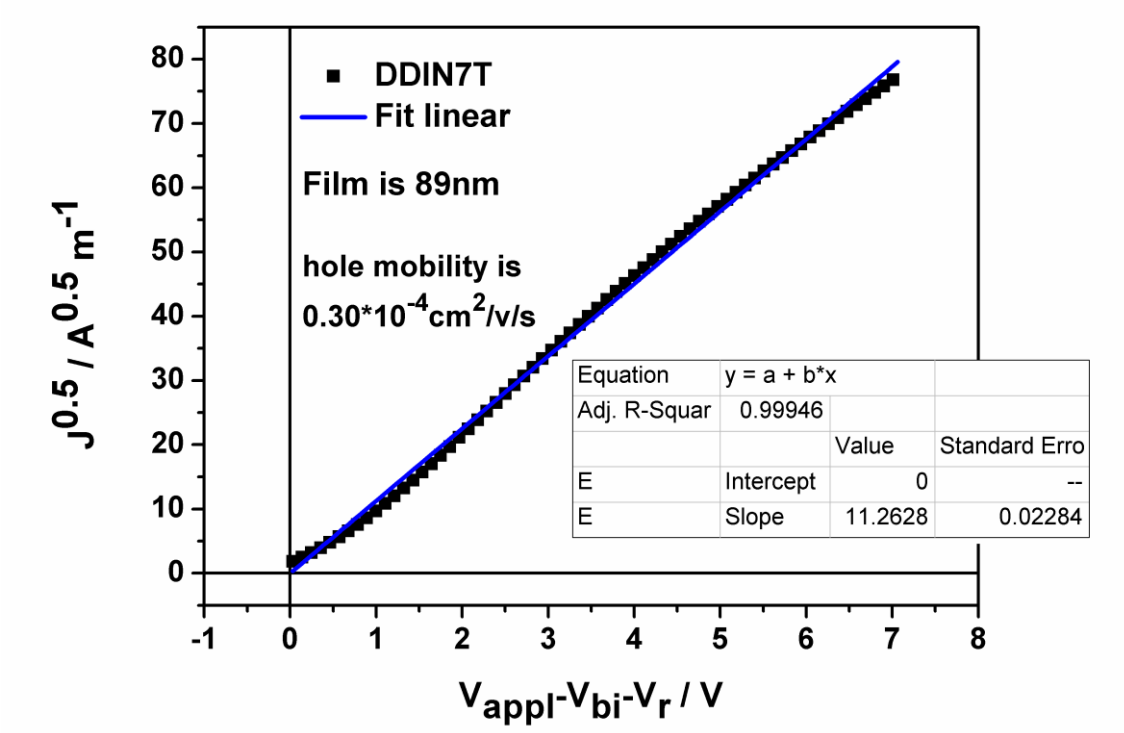

Figure S18. $J^{0.5}$ **vs V plots for the pure DDIN7T film at room temperature.**

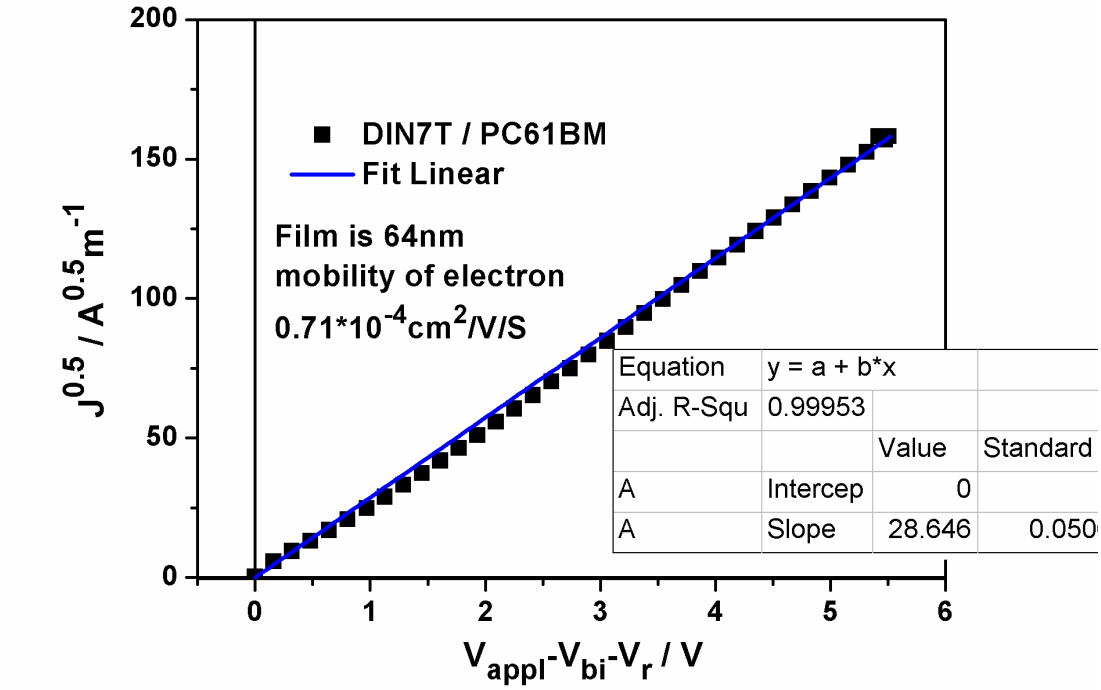

Figure S19. $J^{0.5}$ vs V plots for the DIN7T / PC61BM film at room temperature.

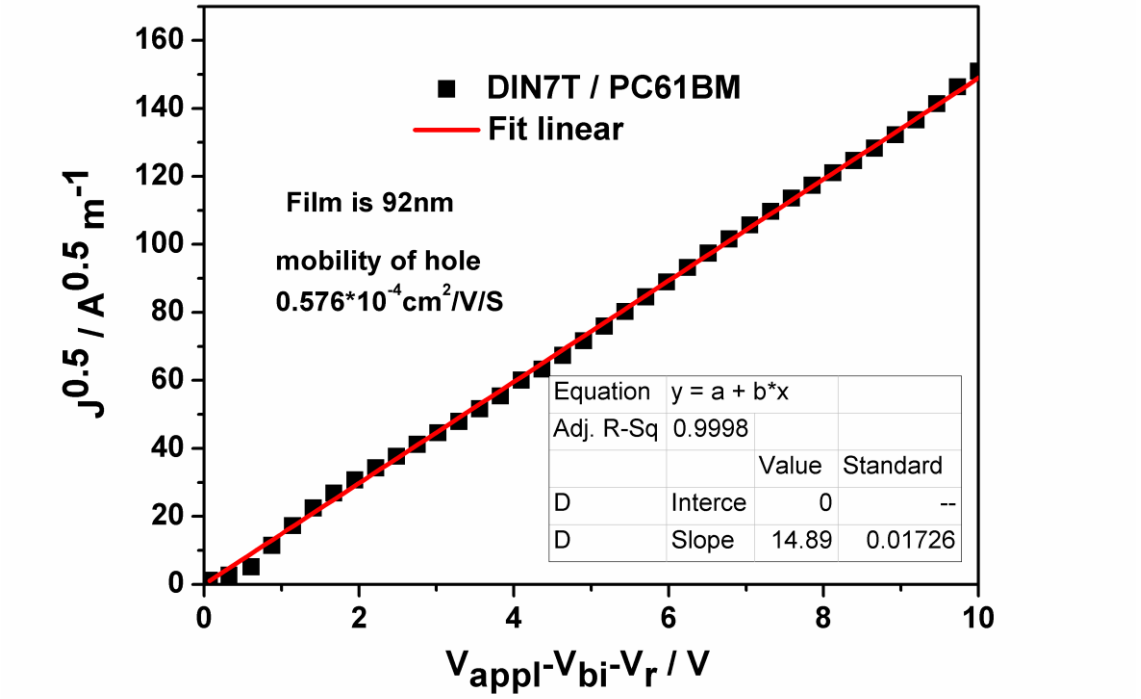

Figure S20. $J^{0.5}$ vs V plots for the DIN7T / PC61BM film at room temperature.

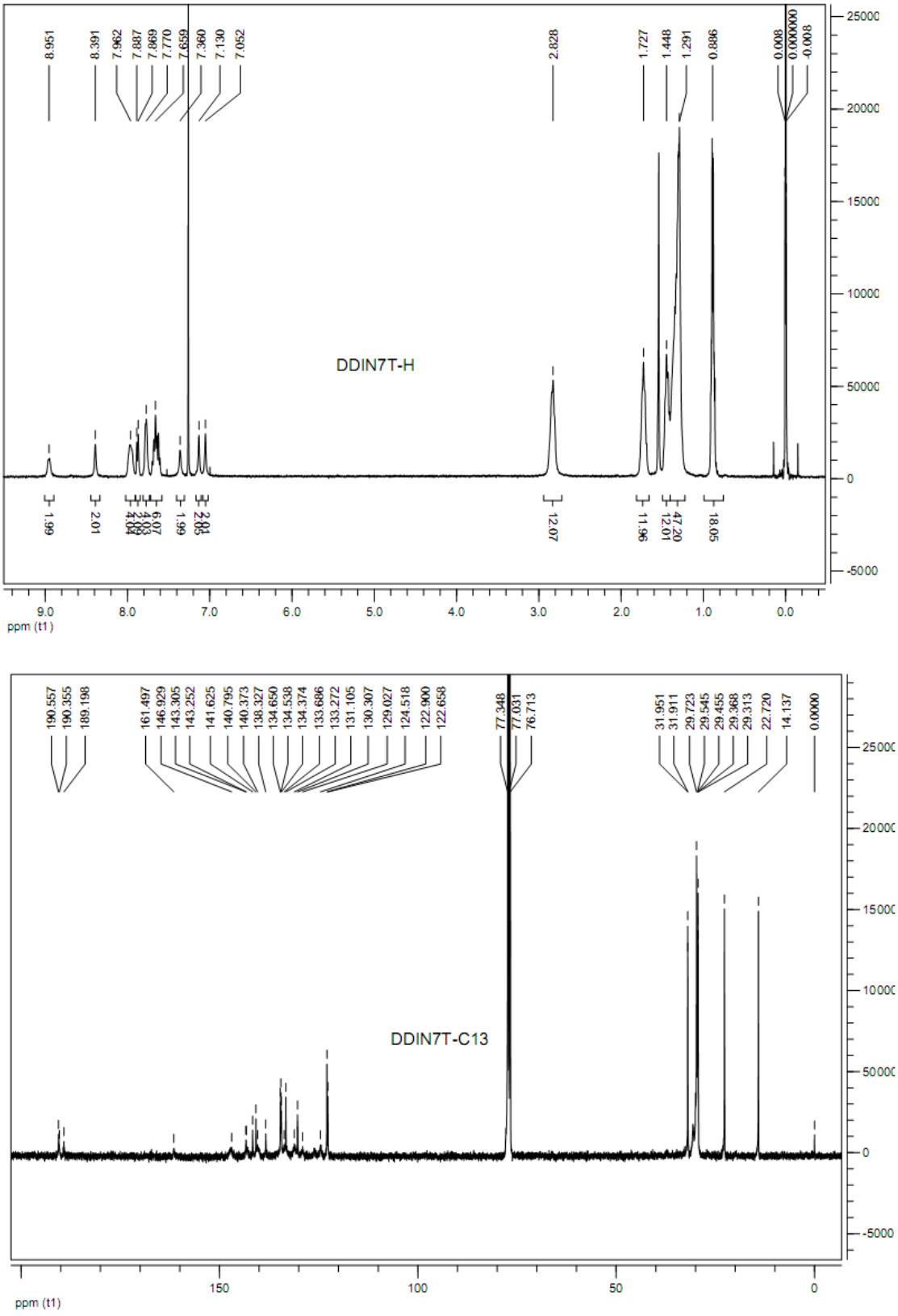

Figure S21. **^{1}H NMR (top) and ^{13}C NMR (below) spectra of DDIN7T.**

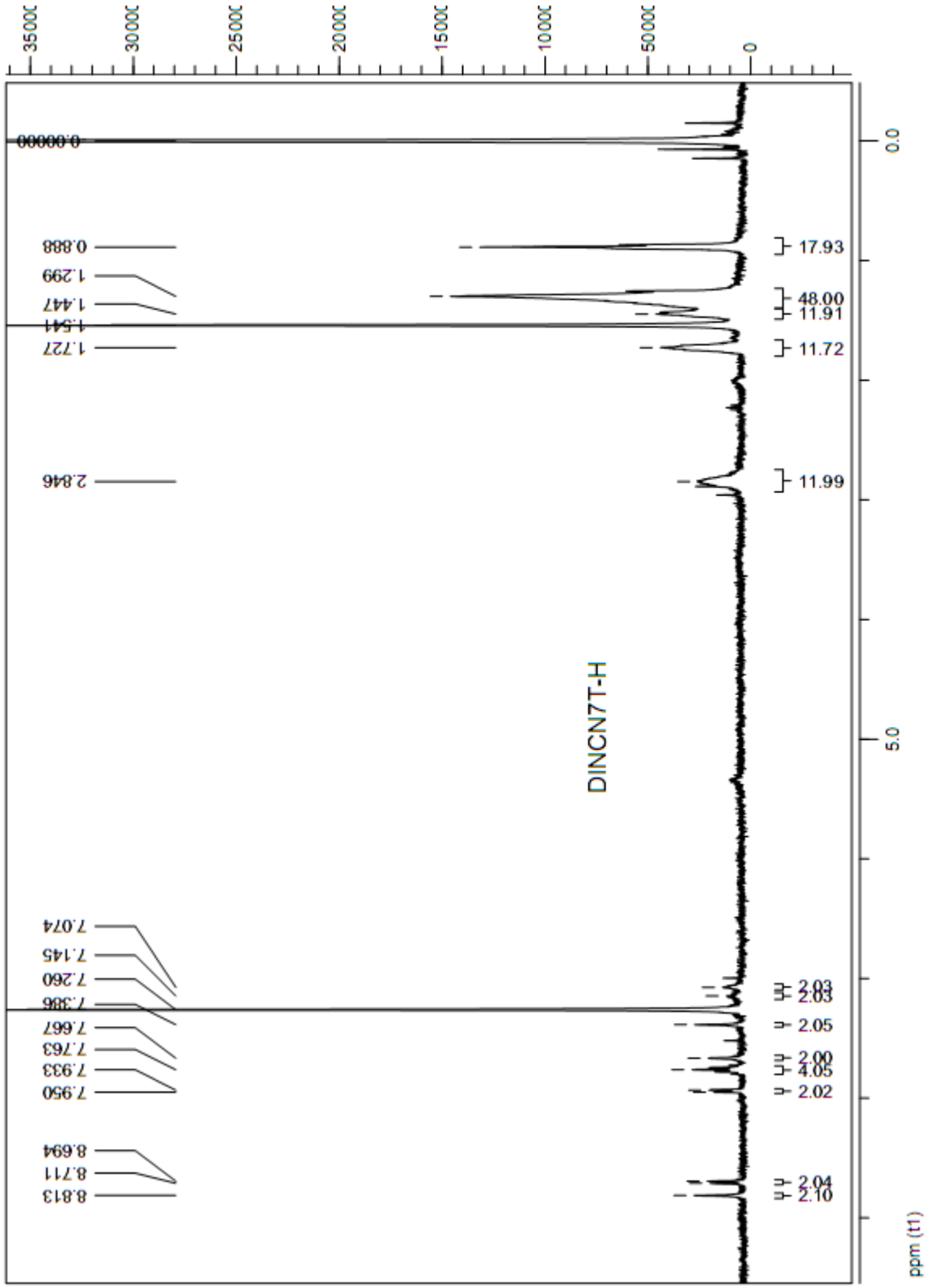

Figure S22. ^{1}**H NMR spectrum of DINCN7T.**

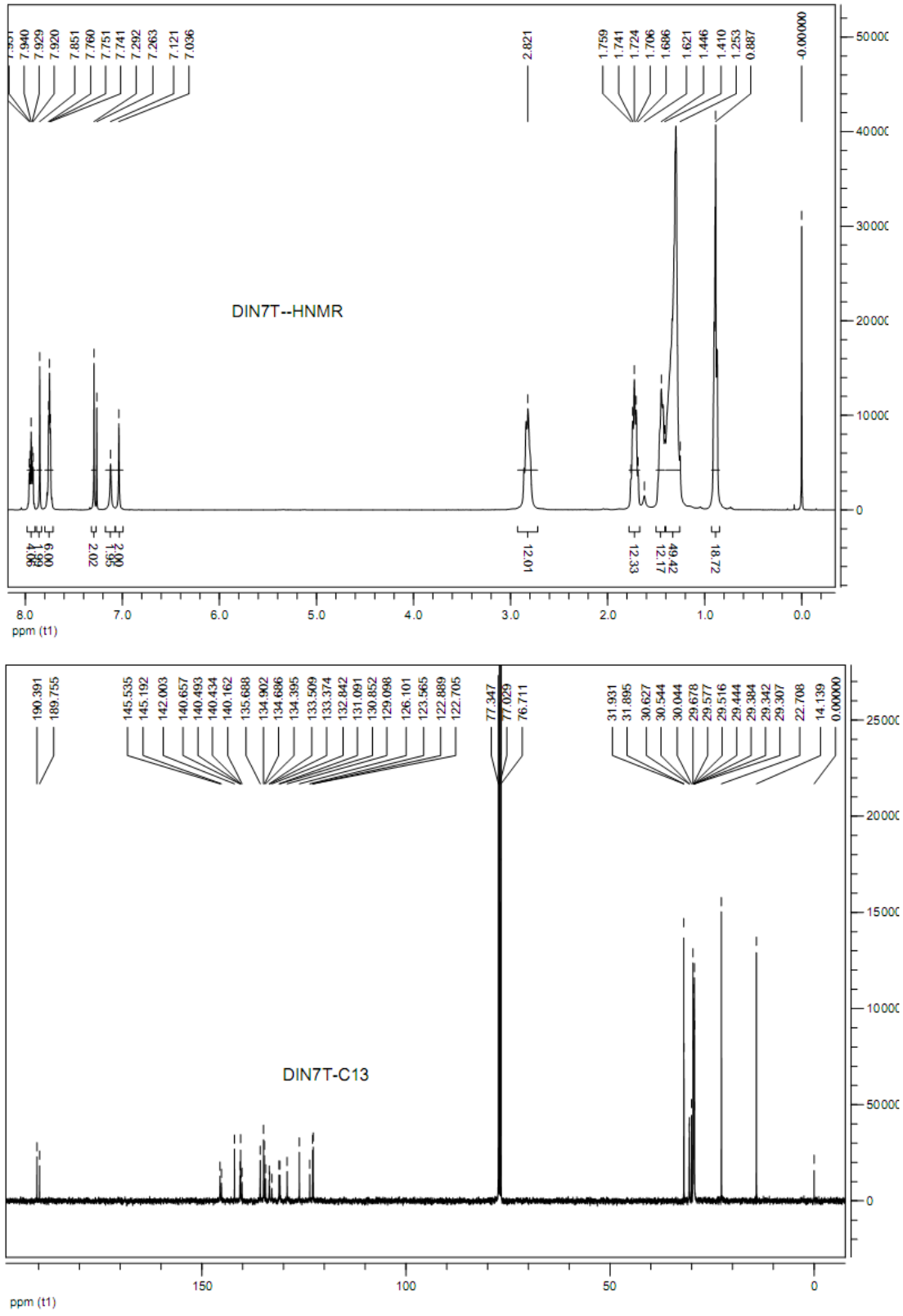

Figure S23. ^{1}H NMR (top) and ^{13}C NMR (below) spectra of DIN7T.

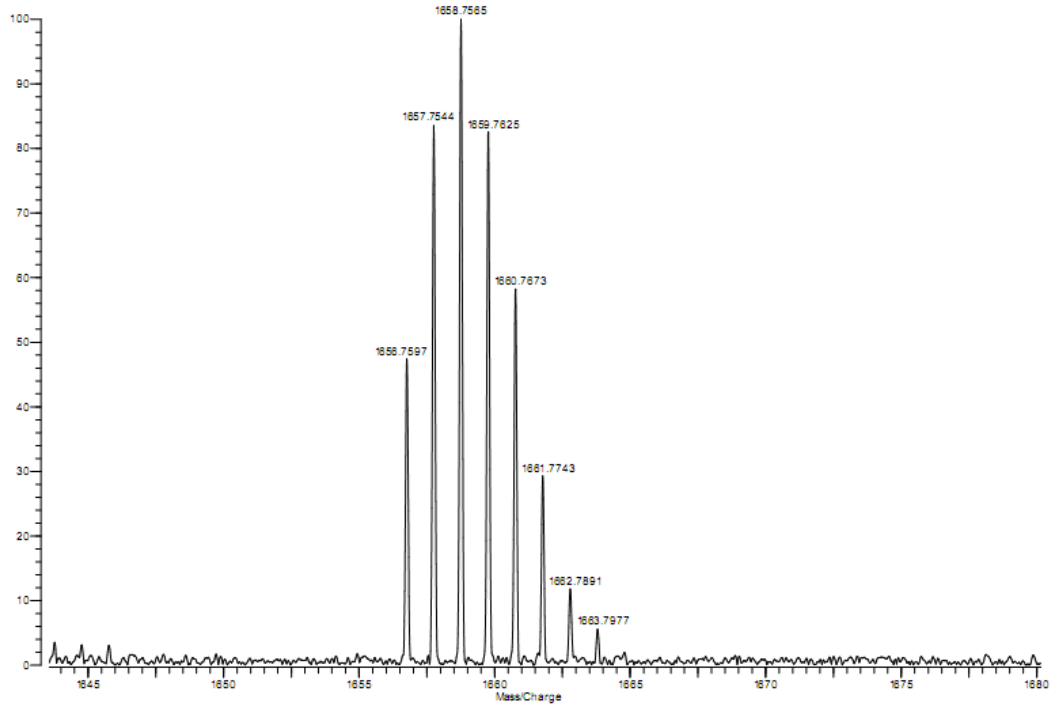

Figure S24. MS (MALDI-FTMS) of DINCN7T

calcd for $C_{102}H_{120}N_4O_2S_7$ $[M]^+$, 1657.7490; found, 1657.7544.

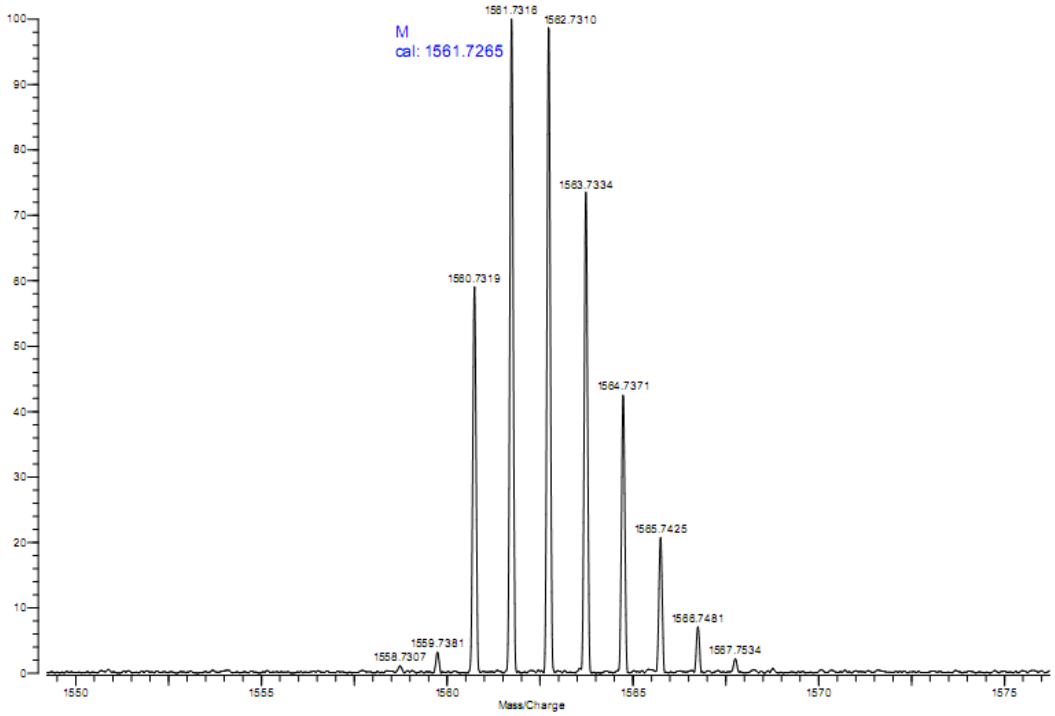

Figure S25. MS (MALDI-FTMS) of DIN7T

calcd for $C_{96}H_{120}O_4S_7$ $[M]^+$, 1561.7265; found, 1561.7316.

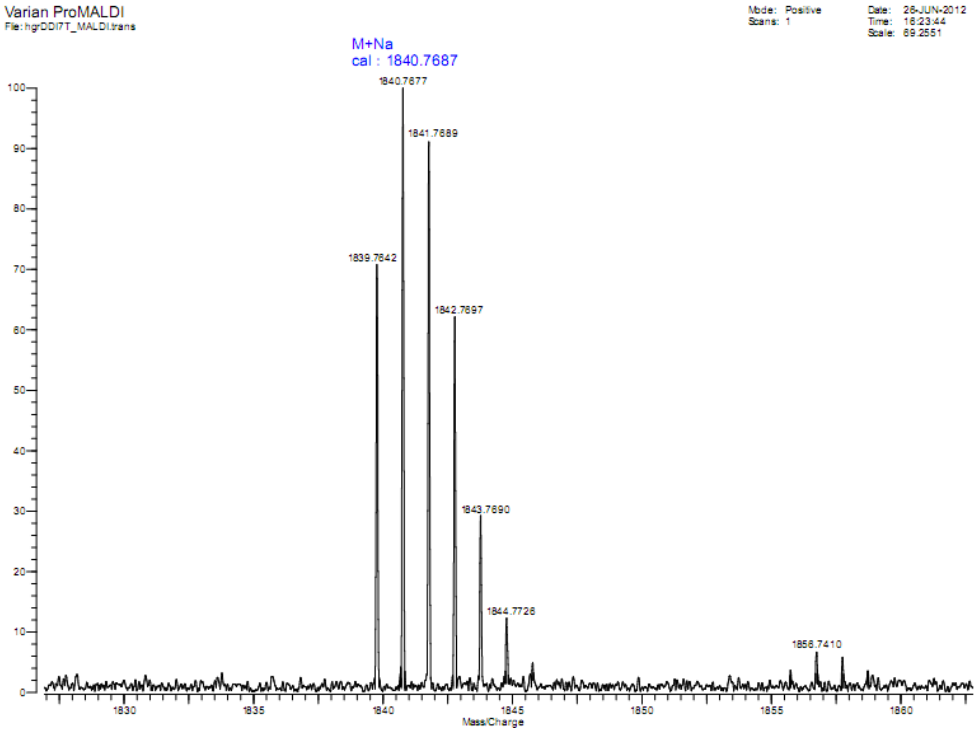

Figure S26. MS (MALDI-FTMS) of DDIN7T
calcd for $C_{90}H_{124}N_4O_6S_7$+Na $[M+Na]^+$, 1840.7667; found, 1840.7677.

---

[1] Absorption coefficient at maximum absorption peaks of D2R(8+2)7T(44---41 L $g^{-1}cm^{-1}$), DTDMP7T(35---43 L $g^{-1}cm^{-1}$), DERHD7T (56---49 L $g^{-1}cm^{-1}$) and DCAO7T (34---40 L $g^{-1}cm^{-1}$) are slight different from reported data(front data highlighted are reported data).

[2] Gaussian 09, Revision B.01,

M. J. Frisch, G. W. Trucks, H. B. Schlegel, G. E. Scuseria, M. A. Robb, J. R. Cheeseman, G. Scalmani, V. Barone, B. Mennucci, G. A. Petersson, H. Nakatsuji, M. Caricato, X. Li, H. P. Hratchian, A. F. Izmaylov, J. Bloino, G. Zheng, J. L. Sonnenberg, M. Hada, M. Ehara, K. Toyota, R. Fukuda, J. Hasegawa, M. Ishida, T. Nakajima, Y. Honda, O. Kitao, H. Nakai, T. Vreven, J. A. Montgomery, Jr., J. E. Peralta, F. Ogliaro, M. Bearpark, J. J. Heyd, E. Brothers, K. N. Kudin, V. N. Staroverov, T. Keith, R. Kobayashi, J. Normand, K. Raghavachari, A. Rendell, J. C. Burant, S. S. Iyengar, J. Tomasi, M. Cossi, N. Rega, J. M. Millam, M. Klene, J. E. Knox, J. B. Cross, V. Bakken, C. Adamo, J. Jaramillo, R. Gomperts, R. E. Stratmann, O. Yazyev, A. J. Austin, R. Cammi, C. Pomelli, J. W. Ochterski, R. L. Martin, K. Morokuma, V. G. Zakrzewski, G. A. Voth, P. Salvador, J. J. Dannenberg, S. Dapprich, A. D. Daniels, O. Farkas, J. B. Foresman, J. V. Ortiz, J. Cioslowski, and D. J. Fox, Gaussian, Inc., Wallingford CT, 2010.